Chemical Science

Accepted Manuscript

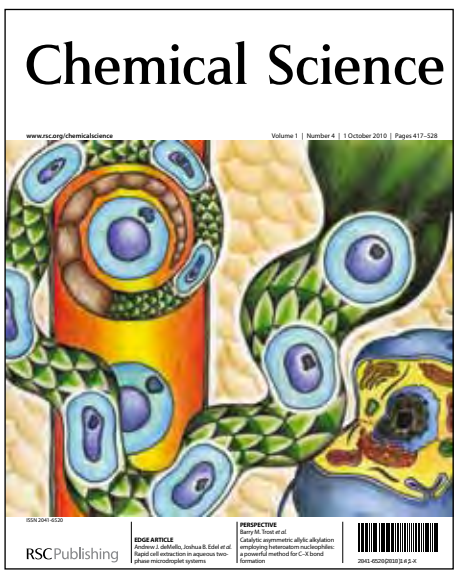

This is an *Accepted Manuscript*, which has been through the RSC Publishing peer review process and has been accepted for publication.

Accepted Manuscripts are published online shortly after acceptance, which is prior to technical editing, formatting and proof reading. This free service from RSC Publishing allows authors to make their results available to the community, in citable form, before publication of the edited article. This *Accepted Manuscript* will be replaced by the edited and formatted *Advance Article* as soon as this is available.

To cite this manuscript please use its permanent Digital Object Identifier (DOI®), which is identical for all formats of publication.

More information about *Accepted Manuscripts* can be found in the **Information for Authors**.

Please note that technical editing may introduce minor changes to the text and/or graphics contained in the manuscript submitted by the author(s) which may alter content, and that the standard **Terms & Conditions** and the **ethical guidelines** that apply to the journal are still applicable. In no event shall the RSC be held responsible for any errors or omissions in these *Accepted Manuscript* manuscripts or any consequences arising from the use of any information contained in them.

Cite this: DOI: 10.1039/c0xx00000x

www.rsc.org/chemicalscience

EDGE ARTICLE

Gold catalyzed hydrogenations of small imines and nitriles: Enhanced reactivity of Au surface toward H_2 via collaboration with a Lewis base

Gang Lu,[a,b] Peng Zhang,[a] Dongqing Sun,[a] Lei Wang,[a] Kebin Zhou,[a] Zhi-Xiang Wang,*[a] and Guo-Cong Guo*[b]

Received (in XXX, XXX) XthXXXXXXXXX 20XX, Accepted Xth XXXXXXXXX 20XX
DOI: 10.1039/b000000x

Clean gold surface is inactive toward H_2, however, the computations, aided by experiments, reveal that gold surface could serve as a Lewis acid coupling with Lewis bases (e.g. imine and nitrile) to construct effective frustrated Lewis pairs (FLPs) to activate H_2 and subsequently to achieve hydrogenation of small imine and nitrile. The Lewis base-coupled Au FLPs avoid tight adsorption of Lewis bases to gold surface via repulsion between nitrogen lone pair and the filled *d*-band electrons of gold surface. This is different from the normal FLPs that use sterically demanding groups or molecular scaffold to prevent formation of stable Lewis acid/base complexes. The enhanced reactivity of the gold surface toward H_2 is due to the synergetic catalytic effects of Lewis acid (Au surface) and the coupled Lewis base (imine or nitrile), which is supported by projected density of states (PDOS) analyses. Among Cu, Ag, and Au surfaces, Au surface exhibits such reactivity most significantly, because Au is much more electronegative than Cu and Ag. The study enriches the FLP chemistry by adding a new type (heterogeneous) of FLPs and reveals a new reaction mode for gold surface.

Introduction

Hydrogenations are important reactions widely used in laboratory synthesis and chemical industry. Because the direct additions of H_2 to unsaturated bonds such as C=C, C=N, and C=O bonds are symmetry-forbidden, hydrogenations using H_2 must be mediated by catalysts. As conventional hydrogenation catalysts, either heterogeneous (e.g. Raney-nickel catalyst[1]) or homogeneous (e.g. metal-ligand bifunctional catalysts[2,3]), involve transition metals (TMs), metal-free systems such as FLPs (frustrated Lewis pairs)[4,5] have recently been found to be capable of activating H_2 facilely. Exemplified by the prototypical FLP, $B(C_6F_5)_3/P(tBu)_3$,[6] a FLP is composed of a Lewis acid and a Lewis base which cannot form a conventional Lewis acid/base adduct because of the sterically demanding substituents. The facile H_2 activation by FLPs is due to the synergetic catalytic effects of the Lewis acid (i.e. $B(C_6F_5)_3$) and the Lewis base (i.e. $PtBu_3$).[7] Since the first report of a FLP, more and more FLPs have been developed. The FLP chemistry has been applied to carry out metal-free hydrogenations,[8-10] to activate other small molecules,[5] and to reduce carbon dioxide to carbon monoxide,[11] methanol,[12] and methane.[13]

The various reported FLPs can be classified as follows: i) homogenous FLPs[6,14-17] (e.g. **A** in Scheme 1) using separate Lewis acid (e.g. B-, Al-centered Lewis acids, or fullerenes) and base (e.g. N-, P-centered Lewis bases, or stable carbenes); ii) homogeneous FLPs[18-23] (e.g. **B**) in which Lewis acidic and basic sites are grafted in a molecular framework; iii) heterogeneous FLPs[24,25] (e.g. **C**, the γ-alumina) where Lewis acidic and basic sites are embedded on the surface of solid; and iv) the FLP concept was initially proposed for metal-free systems, but FLPs using transition metals (TMs) as Lewis acids were also reported[26,27] (e.g. **D**). As the TM Lewis acid and the phosphorus base in **D** are incorporated in one molecule, we computationally showed that the Cp^*Ir intermediate (Lewis acid) can pair with the nitrogen heterocycle to activate H_2 (i.e. **E**)[28] in the reversible dehydrogenation/hydrogenation of nitrogen heterocycle catalyzed by an Ir-complex.[29] It should be pointed out that these FLPs look differently, but all utilize the same principle to achieve high reactivity, that is, using the catalytic effects of Lewis acids and bases simultaneously.[30]

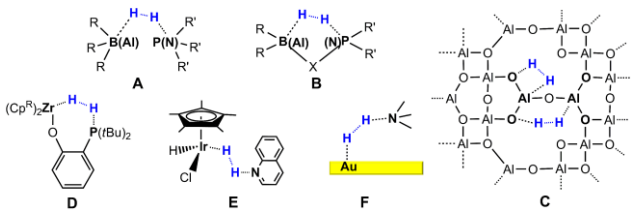

Scheme 1 Types of FLPs (**A~E**) reported previously and the Lewis base-coupled Au FLP (**F**) proposed in the present study. In **A**, fullerene or stable carbene can also serve as Lewis acid or base, respectively. The R and R' represent bulky groups. The X group in **B** represents linkages separating the Lewis acidic and basic sites.

The experimental discovery of FLPs has encouraged computational studies.[7,31-41] We computationally designed metal-free molecules/active sites for hydrogen[42,43] and methane[44] activations and for imine[45,46] and ketone[47] hydrogenations.

Encouragingly, our designed molecules/active sites anticipated features similar to those in the later synthesized compounds.[19,22,23] Related to the metal-free H_2 activation, we further proposed a strategy to integrate the aromatization effect and FLP reactivity to achieve metal-free reversible H_2 activation via the formal [4+2] reaction mode.[48]

Recently, gold catalysis has attracted extensive research interest. Various gold catalysts including gold complexes and nano-gold have been prepared and investigated.[49-53] Aerobic oxidation reactions catalyzed by bulk gold were reported.[54,55] Gold surface covered by pre-adsorbed atoms such as atomic H[56] and O[57,58] or species such as OH[59] could results in various reactions. Nevertheless, probably because of the well-known fact that clean bulk gold surface is inert to H_2,[60] hydrogenation using clean gold surface and H_2 has not been explored. In this study, we report that clean gold surface may serve as a Lewis acid to couple with imine/nitrile to form a new type of heterogeneous FLPs (i.e. **F**) which can activate H_2 and further achieve hydrogenation.

Computational and experimental details

Computational details

All calculations were carried out using the Vienna ab initio simulation package (VASP).[61] The GGA-PW91 density functional[62] was employed to describe electron exchange and correlation, in combination with the projector augmented wave (PAW)[63] function method with plane-wave basis sets (cutoff = 400 eV). The reciprocal space was represented by a 3×3×1 Monkhorst-Pack[64] *k*-point grid. Because the (111) facet is most stable for gold surface, we used the Au(111) facet to represent gold surface. The Au (111) surface was modeled by a four-layer slab, with a *p*(3×3) unit cell in the lateral directions and a vacuum of 16 Å between slabs. The upper two layers were allowed to relax and the atoms in the bottom two layers were fixed at the bulk positions that were taken from the calculated lattice constant of 4.17 Å (the experimental value is 4.08 Å). The dipole correction was considered in the *z* direction. For the optimized structures, the energies were converged to within 10^{-4} eV and the forces were smaller than 0.02 eV/Å. Both spin-polarized and unpolarized calculations were performed when a single H atom is involved in a reaction, and the spin polarization was found to have a negligible impact on the relative energies. Isolated gas-phase molecules were optimized in a (15×15×15 Å) unit cell for small molecules except for $B(C_6F_5)_3/P(tBu)_3$ which used a 30×30×30 Å unit cell. Bader charges of atoms and molecules were computed using the standard method.[65] The transition states (TSs) were optimized by using the climbing-image nudged elastic band method (CI-NEB)[66,67] at a reduced force threshold of 0.05 eV/Å, with eight images between the starting and ending points. All TSs were confirmed by frequency analysis.

Experimental details

N-benzylidenemethylamine and benzonitrile were purchased from Alfa Aesar and the gold powder was purchased from Aladdin. Acetone and toluene were reagent grade and H_2 (≥99.9%) was used as received. Thin layer chromatography was performed using glass plates pre-coated with silica gel (0.25 mm, 60 Å pore size, 230-400 mesh) impregnated with a fluorescent indicator (254 mm). The spots were visualized by exposure to ultraviolet light at 254 nm or under iodine vapor. Column chromatography purifications were performed by flash chromatography using silica gel (200-300 mesh). ^1H and ^{13}C NMR spectra were recorded using a JOEL JNM-ECA600 NMR spectrometer. Mass spectra were recorded on Micromass Platform QP-2010. The total surface area of the gold powder was determined by the BET method using N_2 adsorption at 77 K on a Gemini V. The TEM (transmission electron microscopy) images were obtained by a transmission electron microscopy (Philips CM120).

A mixture of N-benzylidenemethylamine (8.0 mmol, 1.0 g) and gold powder (0.8 g) in toluene (3 mL) was prepared in a glass tube (50 mL). For benzonitrile and acetone, the reactants (4 mL) without additional solvent were mixed with the equal amount of gold powder. The glass tube with the reactant mixture was put into an autoclave. 2.0 MPa H_2 was introduced into the autoclave. The mixture was stirred vigorously (magnetic stir bar) at 50 ℃ for 24 h and then worked up by filtration to remove the gold powder. Products of these reactions were separated and purified by column chromatography and then identified by NMR and mass spectra. The isolated yields were given.

Results and Discussion

It has been well documented that, unlike metal surfaces such as Ni, Cu, and Pt, bulk gold surface is not able to activate H_2.[60] According to FLP principle, we conceived that the reactivity of Au surface toward H_2 could be enhanced by coupling with a Lewis base. Using NH_3 as a probe, we computationally examined the speculation. Fig. 1 shows the energetic and geometric results for the H_2 activation by Au/NH_3 pair. In terms of electronic energy, the complex (**Au_NH$_3$**) is 7.3 kcal mol^{-1} lower than Au + NH_3, compared to the 11.5 kcal mol^{-1} electronic binding energy of $B(C_6F_5)_3/P(tBu)_3$ FLP.[7] Because the electronic binding energy does not account for the entropic penalty of the binding process, the adsorption between NH_3 and Au surface must be very weak if any, meeting the requirement for forming an effective FLP. The repulsion between the NH_3 lone pair and the filled *d*-band electrons of gold surface prevents tight adsorption of NH_3 on Au surface. This is different from regular FLPs which use steric effects such as bulky substituents (e.g. **A** and **B** in Scheme 1) or molecular skeletons (e.g. **B** and **C**) to prevent the formation of the otherwise stable Lewis acid-base adduct.

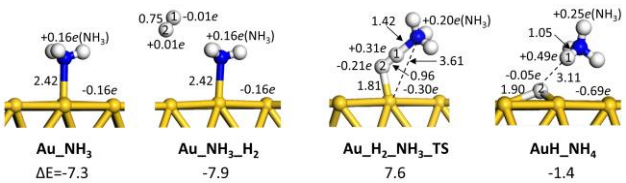

Fig. 1 Optimized structures of the stationary points involved in the H_2 activation by Au/NH_3 pair, along with the key bond lengths (in Å), relative energies to Au + H_2 + NH_3 (ΔE, kcal mol^{-1}), and Bader charge population.

When placing a H_2 molecule close to the **Au_NH$_3$** complex, another local minimum (**Au_NH$_3$_H$_2$**) could be located. The very small charges on the two hydrogen atoms of H_2 moiety (+0.01*e* and -0.01*e*, respectively) and the almost unchanged H-H bond length (0.75 Å, which is the same as that in free H_2) indicate that the H_2 moiety does not effectively interact with either the gold

surface or NH_3. The minimum is only 0.6 kcal mol^{-1} lower than **Au_NH$_3$** + H_2.

In the H_2 activation transition state (TS), **Au_H$_2$_NH$_3$_TS**, the dihydrogen lies between Au surface and NH_3, geometrically similar to the TS for the H_2 activation by FLPs (e.g. $B(C_6F_5)_3/P(t\text{Bu})_3$ FLP[7]). The dihydrogen bond is stretched to 0.96 Å from 0.75 Å in **Au_NH$_3$_H$_2$** and the two hydrogen atoms are 1.81 Å (Au-H[2]) and 1.42 Å(N-H[1]) apart from Au surface and NH_3 moiety, respectively. Relative to **Au_NH$_3$** + H_2, the activation barrier is 14.9 kcal mol^{-1}, which is higher than the H_2 activation barrier (10.4 kcal mol^{-1}) by $B(C_6F_5)_3/P(t\text{Bu})_3$ FLP[7] but less than the value (17.3 kcal mol^{-1}) that is typically considered to be surmountable for surface reactions.[68]

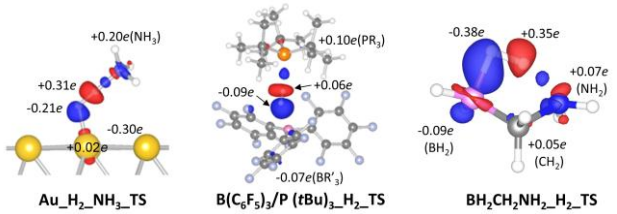

Fig.2 Comparing the charge density difference (Δρ) maps of the H_2 activation TSs by Au/NH_3, $B(C_6F_5)_3/P(t\text{Bu})_3$ and $BH_2CH_2NH_2$ FLPs. Blue and red surfaces denote gain and loss of electron density, respectively. Bader charges are given in black. Note that the charges given in **BH$_2$CH$_2$NH$_2$_H$_2$_TS** are the charge difference between those of the TS and $BH_2CH_2NH_2$.

In agreement with our speculation, the H_2 activation barrier (14.9 kcal mol^{-1}) by Au/NH_3 pair is significantly lower than the barrier (27.6 kcal mol^{-1}, see Fig. S1 in electronic supplementary information for details) by clean Au(111) surface. We investigated the reasons for the decreased barrier. With respect to **Au_NH$_3$_H$_2$**, even though the NH_3 moiety in **Au_H$_2$_NH$_3$_TS** moves further away from Au surface (the shortest N-Au distance increases to 3.61 Å from 2.42 Å), the total negative charge on the Au surface is increased to -0.30*e* from -0.16*e* and the NH_3 moiety donates more electron density (the charge of NH_3 is increased to +0.20*e* from +0.16*e*). The even more significant charge donation from NH_3 to Au surface indicates that the charge transfer is not due to the direct interaction between NH_3 and Au surface, and the middle dihydrogen must play an important role. To understand the role, Fig. 2 compares the charge density difference (Δρ) map of **Au_H$_2$_NH$_3$_TS** with those of the H_2 activation TSs by both inter-moleculear ($B(C_6F_5)_3/P(t\text{Bu})_3$[7]) and intra-molecular ($BH_2CH_2NH_2$) FLPs.[42] It can be observed that the charge transfer patterns in these TSs are very similar. Lewis bases (i.e. NH_3, $P(t\text{Bu})_3$, and NH_2-site) donate electrons to their corresponding Lewis acid partners (i.e. Au, $B(C_6F_5)_3$, and BH_2-site). The H atoms close to Lewis bases bear positive charges (+0.31e, +0.06e, and +0.35e, respectively) and the H atoms bound to Lewis acids have negative charges (-0.21e, -0.09e and -0.38e, respectively). These similarities indicate the dihydrogen plays a similar role in these TSs and thus the reason for the enhanced reactivity of the Au/NH_3 pair toward H_2 is similar to that of FLPs. Overall, the middle dihydrogen in **Au_H$_2$_NH$_3$_TS** bears a net positive charge of +0.10*e*, compared to -0.03*e* in both **B(C$_6$F$_5$)$_3$/P(*t*Bu)$_3$_H$_2$_TS** and **BH$_2$CH$_2$NH$_2$_H$_2$_TS**. The charge difference on the dihydrogen in these TSs reflects the different balance between the electron donation of Lewis base to the H_2 σ*-antibonding orbital and electron withdrawing of Lewis acid (Au surface) from H_2 σ-bonding orbital.

To gain further insight/details into the FLP reactivity of the Au/NH_3 pair in H_2 activation, we analyzed the PDOSs of reactants (H_2, NH_3, Au(111)) and the TS (**Au_H$_2$_NH$_3$_TS**) in Fig. 3. In the reactants, the states corresponding to NH_3 lone pair and σ*(H_2) orbital are localized at around ~0.0 eV and ~10.0 eV, respectively (Fig. 3a1), while the related states in **Au_H$_2$_NH$_3$_TS** delocalize and overlap across -5−0 eV, as shown in Fig. 3a2, which shows a Lewis basic role of NH_3 in activating H_2. Comparing Fig. 3b1 and b2, it is evident that the state of σ(H_2) overlaps with partially filled Au *s*-band at -8.0 eV (Fig. 3b2). Similary, the σ(H_2) state also overlaps with the partially occupied Au *p*-band, but the intensity is much weaker (Fig. 3c1 and c2). These overlaps indicate a Lewis acidic role of Au surface in interacting with H_2 σ electrons. Among the five *d* bands of Au surface, the occupied Au d_z^2 band play a major role in interacting with both σ(H_2) and σ*(H_2) states in **Au_H$_2$_NH$_3$_TS** (Fig. 3d2) and the interactions between other Au *d* states with those of H_2 are negligible (see Fig. S2 for details). The overlap between the Au d_z^2 state and H_2 states signifies two types of interactions including i) the overlap at around -4.5 eV indicates an electron donation from Au filled d_z^2 state to σ*(H_2) state, but the effect could be weak, as shown by the very small positive charge (+0.02*e*, see Fig. 2) on the Au atom bound to the H atom, and ii) the overlaps at around -8.0 eV and -1.0 eV can be attributed to the bonding and anti-bonding interactions between the Au filled d_z^2 state with σ(H_2), respectively. Because both the bonding and anti-bonding overlaps lie below Fermi level and are occupied, these interactions do not contribute to the H_2 activation, as pointed by Nørskov et al.[60] in their study of H_2 cleavage on clean Au(111). In principle, the type ii) overlap is similar to the interaction between two occuiped molecular orbitals when two molecules interact with each other.

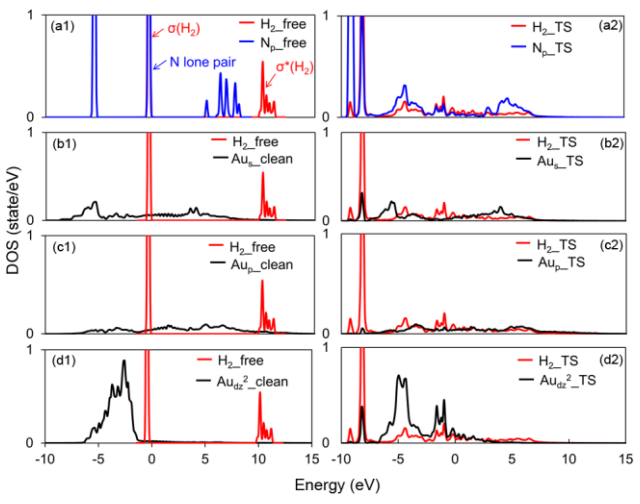

Fig. 3 The PDOS of free H_2, NH_3, clean Au surface and **Au_H$_2$_NH$_3$_TS**. The Fermi level was set at 0.0eV. Note that both the σ(H_2) and N lone pair states appear at ~0.0 eV in (a1).

Summarizing the Δρ map results (Fig. 2) and PDOS analyses (Fig. 3), Scheme 2 depicts the favorbale orbital intractions involved in the H_2 activation by Au(111)/NH_3 pair in a way similar to the fronier molecular orbital (FMO) theory. The NH_3

lone pair and Au d_z^2 state interact with H_2 σ*-antibonding orbital and the partially filled *s*- and *p*-bands of gold interact with H_2 σ-bonding orbital. The former interactions donate electrons to H_2 σ*-antibonding orbital and the latter depletes H_2 σ bonding electrons. Both effects weaken dihydrogen H-H bond, resulting in higher reactivity toward H_2. Note that the Au surface interacts with both σ(H_2) state via its partially filled *s*- and *p*-band (a Lewis acidic effect) and σ*(H_2) state via occupeid d_z^2-band (a Lewis basic effect). However, the Au surface overall plays a Lewis acid role, as demonstrated by the total negative charge (-0.30*e*) on Au surface and its Δρ map which is similar to those of the well-recognized FLPs (Fig. 2).

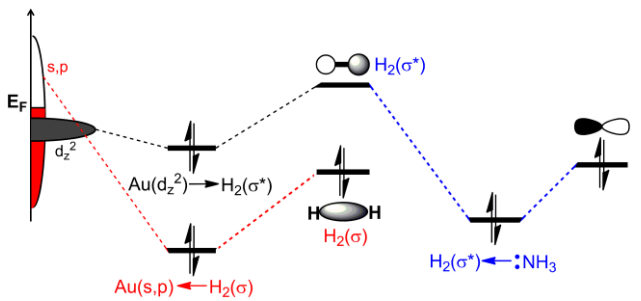

Scheme 2. Schematic illustration of the favorable interactions among Au, H_2 and NH_3.

Similar to the H_2 activation products by normal FLPs, the product **AuH_NH$_4$** can be viewed as an ion pair (i.e. $(AuH)^{\delta-}\cdots(NH_4)^{\delta+}$), as reflected by the charge separation (0.74*e*) on AuH and NH_4 moieties. The H_2 activation by Au/NH_3 is kinetically feasible but thermodynamically unfavorable with the product (**AuH_NH$_4$**) being 6.5 kcal mol^{-1} higher than **Au_NH$_3$_H$_2$**. However, the hydrogen activation can be driven by replacing NH_3 with imine, because imine hydrogenation is thermodynamically favorable, providing driving force for H_2 activation.

The imine hydrogenation can take place by following a mechanism similar to that catalyzed by $B(C_6F_5)_3$.[36] Imine first couples with Au surface to split H_2, then the activated hydrogen atom on Au surface transfers to imine carbon, completing hydrogenation. The hydrogenation mechanism is different from the general hydrogenation using either heterogeneous[1] or regular homogeneous[2,3] catalysts, where the catalysts first activate H_2 independently, giving catalyst hydride, followed by two hydride transfers to the unsaturated bond of substrates. In the present case, the substrate (imine) also plays a crucial role in H_2 activation.

Using Me_2C=NH as an imine model, Fig. 4 shows the computed energetics for the imine hydrogenation on Au(111) surface to give Me_2CH-NH_2, along with the optimized structures of stationary points. The imine (Me_2C=NH) first adsorbs on the Au surface at the top site, forming a complex (**IM1**) with an adsorption energy of 5.1 kcal mol^{-1}. The co-adsorption of H_2 and Me_2C=NH on Au surface giving **IM2** lowers the system by 0.9 kcal mol^{-1}. The transition state (**TS1**) is similar to the **Au_H$_2$_NH$_3$_TS** in Fig. 1, but the length of dihydrogen bond (0.90 Å) is shorter than the 0.96 Å in **Au_H$_2$_NH$_3$_TS**. Consistently, the hydrogen activation barrier (9.8 kcal mol^{-1}) of **TS1** relative to **IM2** is less than the corresponding value (14.9 kcal mol^{-1}) for the H_2 activation by Au/NH_3 pair. After H_2 cleavage, an intermediate (**IM3**) forms, in which the adsorbed hydrogen atom (denoted as H*) lies in the *fcc* site of Au surface. **IM3** is 3.6 kcal mol^{-1} lower than **IM2**, which is in contrast to the NH_3 scenario where **AuH_NH$_4$** is 6.5 kcal mol^{-1} higher than **Au_NH$_3$_H$_2$**. Thus, the H_2 activation by Au/Me_2C=NH FLP pair is more favorable than by Au/NH_3 pair in terms of both kinetics and thermodynamics. The energetic difference between Au/Me_2C=NH and Au/NH_3 pairs could be ascribed to the larger size of Me_2C=NH than NH_3 that benefits stabilization of the cationic species (Me_2C=NH_2^+ versus NH_4^+) in the TS and product.

To transfer H* to the unsaturated carbon of imine, **IM3** adjusts to **IM4** which has more suitable arrangement for H* transfer. The adjustment disturbs the ion pair interaction in **IM3**, placing **IM4** 2.5 kcal mol^{-1} above **IM3**. The surface H* transfers to the carbon of Me_2C-NH_2 after crossing a barrier (**TS2**) of 7.1 kcal mol^{-1} (relative to **IM4**), leading to the complex **IM5** that is 29.5 kcal mol^{-1} more stable than Au(111) + Me_2C=NH + H_2. The adsorption energy of hydrogenation product (Me_2CH-NH_2) on Au surface is only 4.0 kcal mol^{-1}, thus the product can be released easily.

Using HCN as a representative of nitriles, we also explored whether the strategy could be applied to nitrile hydrogenation. Fig. 5 gives the energetic and geometric results for the H_2 addition to HCN giving amine H_3C-NH_2 via two sequential hydrogenation steps. From **IM1b** to **IM5b** in Fig. 5, HCN is hydrogenated to H_2C=NH on Au(111) surface. The barriers of hydrogen activation (**TS1b**) and hydride transfer (**TS2b**) are 16.2 and 10.3 kcal mol^{-1} (relative to **IM4b**), respectively. From **IM6b** to **IM10b**, H_2C=NH is hydrogenated to H_3C-NH_2. The barriers of hydrogen activation (**TS3b**) and hydride transfer (**TS4b**) are 15.7 and 11.6 kcal mol^{-1} (relative to **IM9b**), respectively. The barriers of the two hydrogen activations (**TS1b** and **TS3b**) and hydride transfer (**TS2b** and **TS4b**) are higher than those (9.8 kcal mol^{-1} for **TS1** and 7.1 kcal mol^{-1} for **TS2**) in Me_2C=NH hydrogenation. The higher barriers of HCN hydrogenation could be ascribed to the stronger adsorption of HCN and H_2C=NH due to the smaller steric effects of HCN/H_2C=NH than Me_2C=NH. The strong adsorptions result in favorable thermodynamics; as shown in Fig. 5, the reactions are downhill with all intermediates and transition states lower than Au(111) + HCN. The energetic results indicate that that the Au(111) surface could mediate nitrile hydrogenation either.

The mechanism for imine/nitrile hydrogenation was also explored for ketone hydrogenation. Using Me_2C=O as a ketone representative, Fig. 4 shows the energetics for the hydrogenation of the ketone (Me_2C=O). Because ketone is less Lewis basic than imine, ketone hydrogenation is expected to be less favorable. Indeed, the ketone hydrogenation has a late H_2 activation transition state (**TS1a**) in which the H-H bond length is quite long (2.05 Å). The two barriers (**TS1a** and **TS2a**) in the ketone hydrogenation are 16.8 and 17.2 kcal mol^{-1} higher than the corresponding barriers (**TS1** and **TS2**) in the imine hydrogenation, respectively. Due to the high barriers, Au(111) surface should not be able to catalyze ketone hydrogenation, although ketone hydrogenation is also thermodynamically favorable. Note that the H_2 activaiton barrier (23.6 kcal mol^{-1}) of **TS1a** relative to **IM2a** is also lower than the H_2 activation barrier (27.6 kcal mol^{-1}) by clean gold surface, showing somewhat catalytic effect of the Lewis base (ketone).

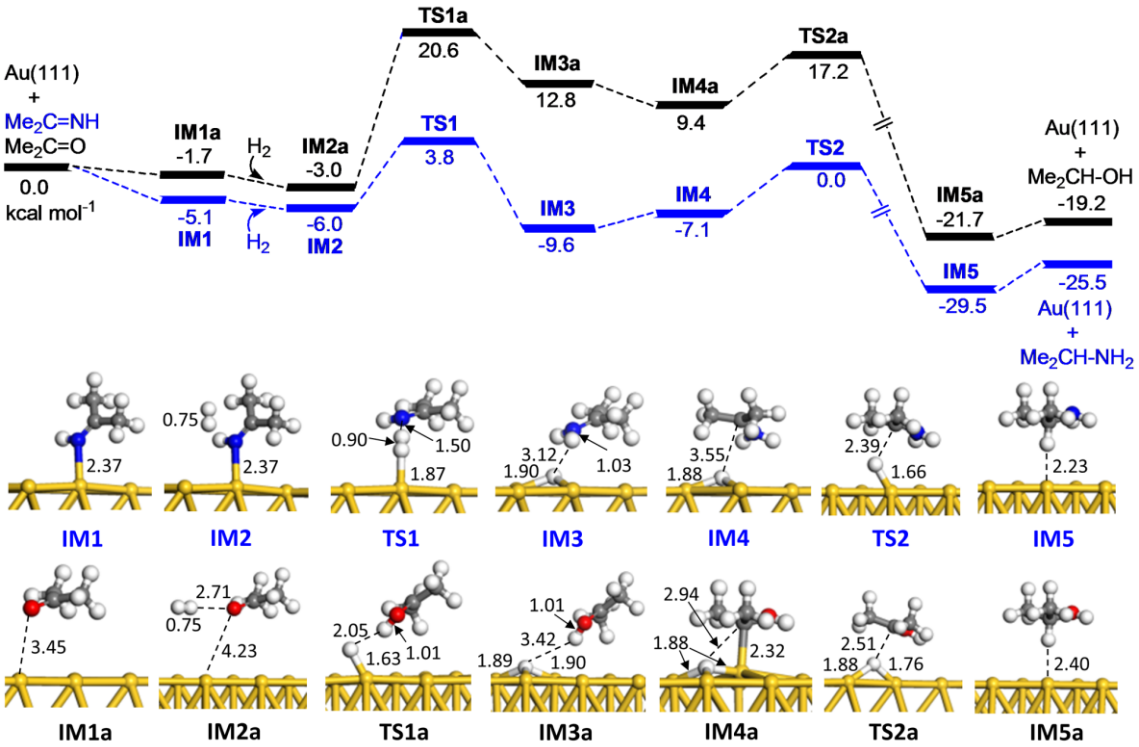

Fig. 4 Energy profile of hydrogenation of $Me_2C=NH$ (blue) and $Me_2C=O$ (black) on the Au(111) surface and the optimized geometries of stationary points, together with the key geometric parameters (Å).

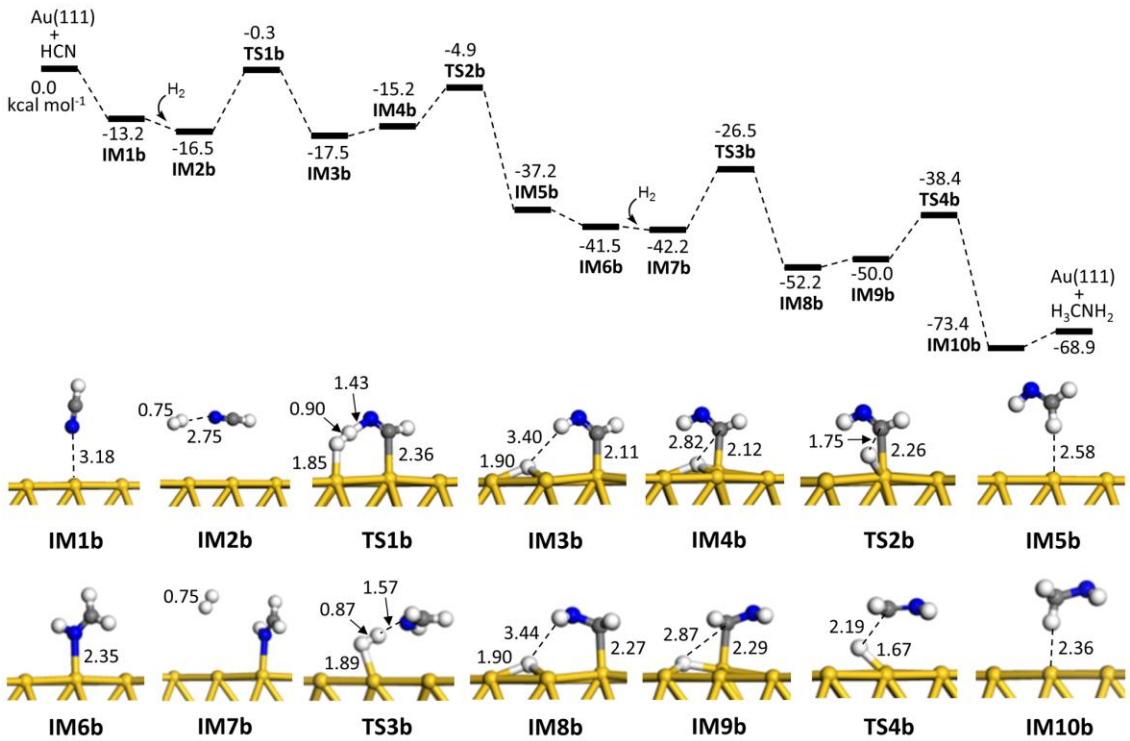

Fig. 5 Energy profile of hydrogenation of HCN to H_3CNH_2 on the Au(111) surface and the optimized geometries of stationary points, together with the key geometric parameters (Å).

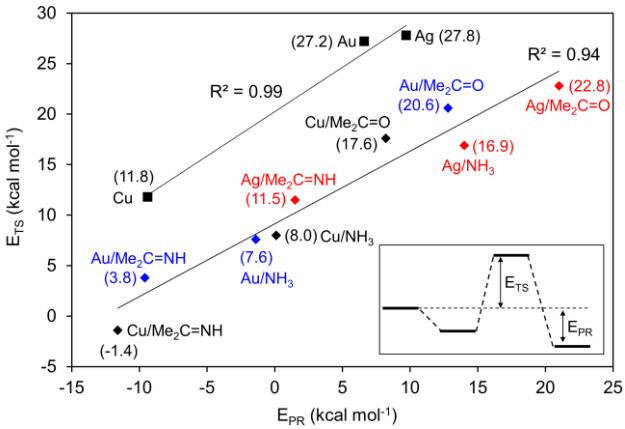

Fig. 6 Relationship between the energies of the TSs (E_{TS}) and the reaction energies (E_{PR}) in the H_2 activations by clean M(111) (M=Cu, Ag, Au) surfaces and M(111)/Lewis bases (Me_2C=NH, NH_3, Me_2C=O). The values in the parentheses are E_{TS}.

We further investigated the reactivity trend twoard H_2 of clean M(111) (M=Cu, Ag, and Au) surfaces and M(111)/Lewis bases (i.e. Me_2C=NH, NH_3, and Me_2C=O) systems. By analogy to the Brønsted−Evans−Polanyi (BEP) plotting, Fig. 6 plots the TS energies of H_2 activation (E_{TS}) versus reaction energies (E_{PR}). It can be observed that the BEP linear relation clearly divides these systems into two groups, including the clean metal surfaces with a R^2=0.99 and the Lewis base-coupled metal surfaces with a R^2=0.94. The division indicates that the coupled Lewis bases alter the H_2 activation pattern by clean metal surfaces, supporting aforementioned FLP reactivity for the Lewis base-coupled Au systems. Except for Cu/Me_2C=O, all the Lewis base-coupled surfaces have smaller E_{TS} than their corresponding clean surfaces, which can be attributed to the catalytic effect of the coupled Lewis bases. When coupled with Lewis bases, Au and Ag surfaces behave similarly but with the former being superior to the latter in reactivity. For both systems, the E_{TS} and E_{PR} increase as the Lewis bases go from Me_2C=NH to NH_3 to Me_2C=O. This trend is in line with the basicity of the Lewis bases and their capability in stabilizing a protonic H in the TSs and prducts. However, Cu surfac behaves differently. Cu/Me_2C=NH and Cu/NH_3 pairs have lower (13.2 and 3.8 kcal mol^{-1}, respectively) E_{TS} than clean Cu surface, but Cu/Me_2C=O has a higher (5.8 kcal mol^{-1}) E_{TS} than clean Cu surface. We rationalize the abnormality of Cu surface as follow. In principle, similar to H_2 activation by transition metal complexes, the driving force for H_2 activation by clean metal surface originates from the synergic effect of bifunctional reactivity (i.e. a metal surface also possesses both Lewis acidic (accepting electrons) and basic (donating electrons) effects). Among the three clean surfaces, Cu surface has a filled *d*-band centered at -2.67 eV, higher than those of Ag at -4.30 eV and Au at -3.56 eV[69]. Because the higher the filled *d*-band, the easier the metal surface donates electrons (i.e. surface Lewis basic effect), the Cu surface has a much lower E_{TS} (11.8 kcal mol^{-1}) for H_2 activation than Ag surface (27.8 kcal mol^{-1}) and Au surface (27.2 kcal mol^{-1}). Thus, the surface Lewis basic effect must play a much more significant role in H_2 cleavage by clean Cu surface than by clean Ag and Au surfaces. Coupling a Lewis base to a clean metal surface brings extra Lewis basic effect, which benefits H_2 cleavage, but meantime it also disturbs the optimal arrangement for metal surface to exert surface Lewis basic effect. This is clear by comparing the TS geometries of the H_2 activation by clean metal surface and Lewis base-coupled metal surface. As exemplified by **TSa** and **TSb** in Figure 7 for H_2 activation by clean Cu surface and Cu/Me_2C=O, respectively, the H_2 moiety in **TSa** is parallel to the metal surface, while the moiety tilts in **TSb**; the former arrangement is more suitable for Cu surface to exercise its own Lewis basic interaction than the latter. If the gain in Lewis basic effect due to the coupled Lewis base is smaller than the lose of surface Lewis basic effect, the E_{TS} of the Lewis base coupled surface would increase. This is the case for Cu/Me_2C=O system, becasuse clean Cu surface already has strong surface Lewis basisc effect (see above) and Me_2C=O is a weak Lewis base. Me_2C=NH and NH_3 are stronger Lewis bases, their Lewis basic effects can surpass the loss of surface Lewis basic effect, thus Cu/Me_2C=NH and Cu/NH_3 systems have reduced E_{TS}. This holds true for all Lewis base-coupled Ag and Au systems, because clean Ag and Au surfaces utilize less surface Lewis basic effect, as indicated by their lower filled *d*-bands (see above). On the other hand, because of the much greater electronegativity of Au (2.43) than those of Cu (1.90) and Ag (1.93), we reasoned that clean Au surface exerts more significant surface Lewis acid effect, which is consistent with the larger surface charge (-0.16*e*) in Au/NH_3 compex than those (-0.08*e*) in Ag/NH_3 and Cu/NH_3 complexes. Therefore, clean Au surface is more Lewis acidic than the other two surfaces and manifests FLP reactivity more significantly. Consistently, couplings of Me_2C=NH, NH_3, and Me_2C=O to Au surface reduce the E_{TS} by 23.4, 19.6, and 6.6 kcal mol^{-1}, respectively, which are larger than the 13.2, 3.8, and -5.8 kcal mol^{-1} for Cu surface and 16.3, 10.9, and 5.0 kcal mol^{-1} for Ag surfce.

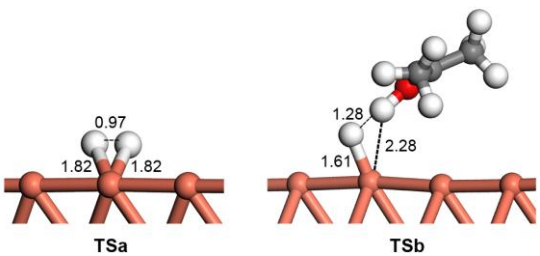

Fig. 7 Geomtries of transiton states for H_2 activation by clean Cu(111) and Cu(111)/Me_2C=O.

The computational results show promise of the hydrogenation strategy. To verify the computational results, the hydrogenation reactions (eq. 1, 2, and 3) were carried out at the conditions of 2 MPa H_2 and 50 ℃, using commercial gold powders without supports as the catalyst. The hydrogenation of benzonitrile to benzylamine passes N-benzylideneamine. N-benzylidenemethylamine (eq. 1) and benzonitrile (eq. 2) can be hydrogenated to the corresponding amines with isolated yields of 38% and 25%, respectively. The products were isolated by column chromatography and identified by NMR and mass spectra (see details in Fig. S3). The control reactions without using gold powder did not occur. Hydrogenation of acetone (eq. 3) under the same condition gave no alcohol product, in agreement with the predicted energetics which shows ketone hydrogenation is kinetically much unfavorable (see Fig. 4) than imine/nitrile hydrogenation. The TEM measurements before and after

reactions showed that gold particles have diameters longer than 50 nm (Fig. S4). The gold powder has a surface area of ca. 1.27 m^2 g^{-1} that is significantly less than that of nano-gold catalysts (e.g. ca. 40−50 m^2 g^{-1} of commercial AURO*lite* with the average gold size of ca. 2−3 nm[70]). The TOFs for hydrogenations of N-benzylidenemethylamine (eq. 1) and benzonitrile (eq. 2) were estimated to be 0.0021 s^{-1} and 0.0067 s^{-1}, respectively. Expectedly, the values are smaller than those for the hydrogenations mediated by supported nano-gold catalysts (e.g. 0.045 s^{-1} for acrolein hydrogenation catalyzed by Au/ZrO_2 catalyst[71]). Considering the small surface area and that the reactions involved solid, liquid, and gas three phases, the low isolated yields of hydrogenation products are understandable.

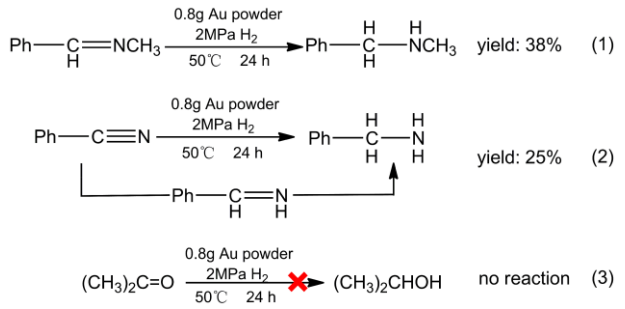

While we attribute the observed catalytic activity of Au surface (i.e. eq. 1 and eq. 2) to the FLP reactivity, we also considered the possibility that the catalytic activity may be due to H_2 acivation by the low-coordinated steps, corners, and defects that may exist in gold powder. While it is difficult to exclude the possibility experimentally, we exclude the possibility to be a major factor by following reasons. If the steps, corners, and defects on gold surface were indeed majorly responsible for the observed hydrogenations (eq. 1 and 2 reactions), the hydrogenation would follow the mechanism: molecular hydrogen is first activated by these low-coordinated steps, corners, and defects, and the activated hydrogen atoms then transfer to the unsaturated bonds (i.e. C=N in eq. 1 or C≡N in eq. 2) of substrates. In this mechanism, the H_2 activation should also take place in ketone hydrogenation (i.e. eq. 3). Therefore, eq. 3 reaction should proceed, which is in disagreement with the experimental observation that eq. 3 reaction did not occur. In contrast, the FLP-based mechanism can rationalize the experimental observation very well. Because ketone is less Lewis basic than imine or nitrile, the ketone in eq. 3 cannot form effective FLP to activate H_2, thus no hydrogenation product can be observed in eq. 3. On the basis of the above reasoning, we conclude that the low-coordinated steps, corners, and defects in gold powder are not the major cause for our observed hydrogenation. In addition, we also reason that Au nanoparticles do not contribute to the observed hydrogenation although they can catalyze various kinds of reactions.[52,53,72] Because Au nanoparticles can easily aggregate, they should be always prepared meticulously and must be supported by supports (such as titania and ceria)[73,74] or protected by organic ligands (such as $-PPh_3$ and thiolate −SR groups)[75,76] to avoid aggregation/deactivation. In our study, we just used commercial Au powder without any processing and no supports or protected ligands. Thus it is highly unlikely that there existed appreciable Au nanoparticles in Au powder to play a major role to promote observed hydrogenations.

To form an effective normal FLP, the Lewis acid and base components should be bulky enough to avoid forming stable Lewis acid/base adducts. This requirement limits applications of FLPs for hydrogenations of small imines (e.g. the NH- or NCH_3-type imines) directly. The use of gold surface as the Lewis acid to construct FLP can circumvent the problem, because stable Lewis acid-base adduct can be avoided intrinsically by the repulsion between nitrogen lone pair and the filled *d*-band electrons of gold. Note that the smallest NH_3 even cannot be adsorbed on the Au surface tightly (see above). Nitriles may be too small to construct normal FLPs due to the highly exposed nitrogen atom, but benzonitrile can be hydrogenated on the Au surface directly. In the imine hydrogenation catalyzed by conventional transition metal catalysts, the formation of Werner-type complexes between imines/or amine products and metal centers make hydrogenations of small imine challenging, because such complexes could deactivate the catalysts. On the gold surface, the small imine (e.g. eq. 1) can be hydrogenated without side reactions. On the other hand, the N-H bond in NH-type imines or amine products may undergo oxidation to break the N-H bond, resulting in side products or catalyst deactivation. As indicated by the energetics shown in Fig. S5, the N-H bond, as well as O-H bond, cannot undergo such oxidations. The activation barriers for N-H bonds of $Me_2C=NH$ and Me_2CHNH_2 and O-H bond of Me_2CHOH on Au(111) surface were calculated to be as high as 43.9, 51.8 and 43.6 kcal mol^{-1}, respectively, which are in agreement with previous experimental[58,59] and theoretical[59,77] studies.

Conclusions

In summary, the computational study, aided by experimental study, shows that Au(111) surface can serve as a Lewis acid to couple with imine/nitrile to activate H_2 and further to realize hydrogenation. The Lewis base-coupled Au FLPs utilize the synergetic catalytic effects of Lewis acids and bases to achieve high reactivity toward H_2, but distinguish from the normal FLPs in the four aspects: a) Instead of using bulky substituents or molecular skeletons to prevent the formation of stable Lewis acid/base adducts by normal FLPs, the Lewis base-coupled Au FLPs avoid tight adsorption by using the repulsion between N lone pair and the filled *d*-band electrons of gold surface; b) except for the Lewis basic effect of ammonia/imine/nitrile, the Au d_z^2 state also donates electron to H_2 σ*-antibonding orbital, but the net effect of Au surface plays a role as a Lewis acid; c) instead of using localized Lewis acid site in normal FLPs, it uses the partially filled *s*- and *p*-band to accept the electrons from the H_2 bonding σ orbital; d) among Cu, Ag, and Au surfaces, Au surfaces exhibit such reactivity most significantly, because Au is much more electronegative than Cu and Ag. Because of these characteristics, the approach could be applicable to realize the hydrogenation of small NH- or NCH_3-type imines and nitriles directly, extending the applications of FLP principle to hydrogenate small imine and nitrile.

Acknowledgements

This study was supported by the Chinese Academy of Sciences, NSFC (No. 21173263, 21303203, and 21373216) and the 973 Program (2011CBA00505).

Notes and references

[a]College of Chemistry and Chemical Engineering, University of Chinese Academy of Sciences, Beijing, 100049, P. R. China
[b]State Key Laboratory of Structural Chemistry, Fujian Institute of Research on the Structure of Matter, Chinese Academy of Sciences, Fuzhou, Fujian 350002, P. R. China
E-mail: zxwang@ucas.ac.cn; gcguo@fjirsm.ac.cn

† Electronic Supplementary Information (ESI) available: Geometries and energetics for the activations of H-H, N-H and O-H bonds on Au(111), the PDOS of H_2 and Au states in the transition state, spectroscopic data for the synthesized amines, and TEM images of the gold powder. See DOI: 10.1039/b000000x/

1 S. Nishimura, in *Handbook of Heterogeneous Catalytic Hydrogenation for Organic Synthesis*, John Wiley & Sons, Inc. New York, 2001, pp. 7.
2 R. Noyori and T. Ohkuma, *Angew. Chem., Int. Ed.*,2001, **40**, 40.
3 S. E. Clapham, A. Hadzovic and R. H. Morris, *Coord. Chem. Rev.*, 2004, **248**, 2201.
4 G. C. Welch, R. R. S. Juan, J. D. Masuda and D. W. Stephan, *Science*, 2006, **314**, 1124.
5 D. W. Stephan and G. Erker, *Angew. Chem., Int. Ed.*, 2010, **49**, 46.
6 G. C. Welch and D. W. Stephan, *J. Am. Chem. Soc.*, 2007,**129**, 1880.
7 T. A. Rokob, A. Hamza, A. Stirling, T. Soos and I. Papai, *Angew. Chem., Int. Ed.*, 2008,**47**, 2435.
8 D. W. Stephan, *Org. Biomol. Chem.*, 2012, **10**, 5740.
9 K. Chernichenko, A. Madarasz, I. Papai, M. Nieger, M. Leskela, and T. Repo, *Nat. Chem.*, 2013, **5**, 718.
10 Y. Liu, and H. Du, *J. Am. Chem. Soc.* 2013, **135**, 6810.
11 G.Menard and D. W.Stephan, *Angew. Chem., Int. Ed.*,2011, **50**, 8396.
12 G. Menard and D. W. Stephan, *J. Am. Chem. Soc.*,2010, **132**, 1796.
13 A. Berkefeld, W. E. Piers and M. Parvez, *J. Am. Chem. Soc.*, 2010, **132**, 10660.
14 V. Sumerin, F. Schulz, M. Nieger, M. Leskelae, T. Repo and B. Rieger, *Angew. Chem., Int. Ed.*, 2008, **47**, 6001.
15 D. Holschumacher, T. Bannenberg, C. G. Hrib, P. G. Jones and M. Tamm, *Angew. Chem., Int. Ed.*, 2008, **47**, 7428.
16 H. Li, C. Risko, J. H. Seo, C. Campbell, G. Wu, J.-L. Bredas, and G. C. Bazan, *J. Am. Chem. Soc.*, 2011, **133**, 12410.
17 J. Iglesias-Sigueenza and M. Alcarazo, *Angew. Chem., Int. Ed.*, 2012, **51**, 1523.
18 V. Sumerin, F. Schulz, M. Atsumi, C. Wang, M. Nieger, M. Leskela, T. Repo, P. Pyykko and B. Rieger, *J. Am. Chem. Soc.*, 2008, **130**, 14117.
19 J. Boudreau, M. A. Courtemanche and F. G. Fontaine, *Chem. Commun.*, 2011, **47**, 11131.
20 P. Spies, G. Erker, G. Kehr, K. Bergander, R. Froehlich, S. Grimme and D. W. Stephan, *Chem. Commun.*,2007, **47**, 5072.
21 S. J. Geier, T. M. Gilbert and D. W. Stephan, *J. Am. Chem. Soc.*, 2008, **130**, 12632.
22 E. Theuergarten, D. Schluens, J. Grunenberg, C. G. Daniliuc, P. G. Jones and M. Tamm, *Chem. Commun.*, 2010, **46**, 8561.
23 F. Bertini, V. Lyaskovskyy, B. J. J. Timmer, F. J. J. de Kanter, M. Lutz, A. W. Ehlers, J. C. Slootweg and K. Lammertsma, *J. Am. Chem. Soc.*, 2011, **134**, 201.
24 R. Wischert, C. Coperet, F. Delbecq and P. Sautet, *Angew. Chem., Int. Ed.*, 2011, **50**, 3202.
25 R. Wischert, P. Laurent, C. Coperet, F. Delbecq and P. Sautet, *J. Am. Chem. Soc.*, 2012, **134**, 14430.
26 A. M. Chapman, M. F. Haddow and D. F. Wass, *J. Am. Chem. Soc.*, 2011, **133**, 18463.
27 A. M. Chapman, M. F. Haddow and D. F. Wass, *J. Am. Chem. Soc.*, 2011, **133**, 8826.
28 H. Li, J. Jiang, G. Lu, F. Huang and Z.-X. Wang, *Organometallics*, 2011, **30**, 3131.
29 R. Yamaguchi, C. Ikeda, Y. Takahashi and K. Fujita, *J. Am. Chem. Soc.*, 2009, **131**, 8410.
30 Z.-X. Wang, L. Zhao, G. Lu, H. Li, and F. Huang, in *Frustrated Lewis Pairs I: Uncovering and Understanding*, Eds.: G. Erker and D. W. Stephan, 2013, **332**, 231.
31 T. A. Rokob, I. Bako, A. Stirling, A. Hamza, and I. Papai, *J. Am. Chem. Soc.*, 2013, **135**, 4425.
32 S. Grimme, H. Kruse, L. Goerigk and G. Erker, *Angew. Chem., Int. Ed.*, 2010, **49**, 1402.
33 T. Wiegand, H. Eckert, O. Ekkert, R. Frohlich, G. Kehr, G. Erker and S. Grimme, *J. Am. Chem. Soc.*, 2012, **134**, 4236.
34 Z. P. Lu, Z. H. Cheng, Z. X. Chen, L. H. Weng, Z. H. Li and H. D. Wang, *Angew. Chem., Int. Ed.*, 2011, **50**, 12227.
35 Y. Guo and S. Li, *Inorg. Chem.*, 2008, **47**, 6212.
36 T. A. Rokob, A. Hamza, A. Stirling and I. Papai, *J. Am. Chem. Soc.*, 2009, **131**, 2029.
37 T. A. Rokob, A. Hamza and I. Papai, *J. Am. Chem. Soc.*, 2009, **131**, 10701.
38 H. Li, L. Zhao, G. Lu, Y. Mo and Z.-X. Wang, *Phys. Chem. Chem. Phys.*, 2010, **12**, 5268.
39 T. Privalov, *Chem.-Eur. J.*, 2009, **15**, 1825.
40 H. W. Kim and Y. M. Rhee, *Chem.-Eur. J.*, 2009, **15**, 13348.
41 R. Rajeev and R. B. Sunoj, *Chem.-Eur. J.*, 2009, **15**, 12846.
42 Z.-X. Wang, G. Lu, H. Li and L. Zhao, *Chin. Sci. Bull.*, 2010, **55**, 239.
43 G. Lu, H. Li, L. Zhao, F. Huang and Z.-X. Wang, *Inorg. Chem.*, 2010, **49**, 295.
44 G. Lu, L. Zhao, H. Li, F. Huang and Z.-X. Wang, *Eur. J. Inorg. Chem.*, 2010, **15**, 2254.
45 L. Zhao, H. Li, G. Lu and Z.-X. Wang, *Dalton Trans.*, 2010, **39**, 4038.
46 L. Zhao, H. Li, G. Lu, F. Huang, C. Zhang and Z.-X. Wang, *Dalton Trans.*, 2011, **40**, 1929.
47 H. Li, L. Zhao, G. Lu, F. Huang and Z.-X. Wang, *Dalton Trans.*, 2010, **39**, 5519.
48 G. Lu, H. Li, L. Zhao, F. Huang, P. v. R. Schleyer and Z.-X. Wang, *Chem.-Eur. J.*, 2011, **17**, 2038.
49 A. S. K.Hashmi and G. J. Hutchings, *Angew. Chem., Int. Ed.*, 2006, **45**, 7896.
50 A. Corma, A. Leyva-Perez and M. J. Sabater, *Chem. Rev.*, 2011, **111**, 1657.
51 C. D. Pina, E. Falletta and M. Rossi, *Chem. Soc. Rev.*, 2012, **41**, 350.
52 Y. Zhang, X. Cui, F. Shi and Y. Deng, *Chem. Rev.*, 2012, **112**, 2467.
53 M. Stratakis and H. Garcia, *Chem. Rev.*,2012, **112**, 4469.
54 M. Lazar and R. J. Angelici, *J. Am. Chem. Soc.*, 2006, **128**, 10613.
55 R. J. Angelici, *Catal. Sci.Tech.* 2013, **3**, 279.
56 M. Pan, A. J. Brush, Z. D. Pozun, H. C. Ham, W. Y. Yu, G. Henkelman, G. S. Hwang, C. B. Mullins, *Chem. Soc. Rev.* 2013, **42**, 5002.
57 J. Gong, *Chem. Rev.*, 2012, **112**, 2987.
58 B. Xu, X. Liu, J. Haubrich and C. M. Friend, *Nat. Chem.*, 2010, **2**, 61.
59 B. N. Zope, D. D. Hibbitts, M. Neurock and R. J. Davis, *Science*, 2010,**330**, 74.
60 B. Hammer and J. K. Nørskov, *Nature*, 1995, **376**, 238.
61 G. Kresse and J. Furthmuller, *Phys. Rev. B*, 1996, **54**, 11169.
62 J. P. Perdew, K. Burke and M. Ernzerhof, *Phys. Rev. Lett.*, 1996, **77** 3865.
63 P. E. Blochl, *Phys. Rev. B*, 1994, **50**, 17953.
64 H. J. Monkhorst and J. D. Pack, *Phys. Rev. B*, 1976, **13**, 5188.
65 W. Tang, E. Sanville and G. Henkelman, *J. Phys.: Condens. Matter*, 2009, **21**, 084204.
66 G. Henkelman and H. Jonsson, *J. Chem. Phys.*, 2000, **113**, 9978.
67 G. Henkelman, B. P. Uberuaga and H. Jonsson, *J. Chem. Phys.*, 2000, **13**, 9901.
68 C. Shang and Z.-P. Liu, *J. Am. Chem. Soc.*, 2011, **133**, 9938.
69 A. Nilsson, L. G. M. Petterssonin and J. K. Nørskov, in *Chemical Bonding at Surfaces and Interfaces*, Elsevier, Amsterdam, 2008, pp. 268.
70 D. Preti, C. Resta, S. Squarcialupi and G. Fachinetti, *Angew. Chem., Int. Ed.*, 2011, **50**, 12551.
71 P. Claus, *Appl. Catal. A: Gen.*, 2005, **291**, 222.
72 C. Mohr, H. Hofmeister, J. Radnik and P. Claus, *J. Am. Chem. Soc.*, 2003, **125**, 1905.
73 M. Haruta, T. Kobayashi, H. Sano, and N. Yamada, *Chem. Lett.*, 1987, **16**, 405.
74 G. J. Hutchings, *Catal. Today*, 2005, **100**, 55.
75 G. Schmid, *Chem. Soc. Rev.*, 2008, **37**, 1909.

76 P. D. Jadzinsky, G. Calero, C. J. Ackerson, D. A. Bushnell and R. D. Kornberg, *Science*, 2007, **318**, 430.
77 B. Xu, J. Haubrich, T. A. Baker, E. Kaxiras and C. M. Friend, *J. Phys. Chem. C*, 2011, **115**, 3703.